Synthesis, Characterization, and Partial Hydrolysis of Polyisoprene-*co*-Poly(*tert*-butyl methacrylate) and Electrorheological Properties of Its Suspensions

Mustafa Yavuz,[1] Halil Ibrahim Ünal[2]

[1]*Chemistry Department, Science and Arts Faculty, Süleyman Demirel University, 32260 Isparta, Turkey*
[2]*Chemistry Department, Science and Arts Faculty, Gazi University, 06500 Teknikokullar, Ankara, Turkey*

Received 5 September 2002; accepted 17 June 2002

ABSTRACT: The synthesis, characterization, partial hydrolysis, and salt formation of polyisoprene-*co*-poly(*tert*-butyl methacrylate) and the electrorheological properties of its suspensions were investigated. The copolymer was characterized by gel permeation chromatography, viscosity measurements, ^{1}H-NMR, Fourier transform infrared spectroscopy, particle size measurements, and elemental analysis. The poly(*tert*-butyl methacrylate) units of the copolymer were partially hydrolyzed by *p*-toluene sulfonic acid monohydrate and then converted into a lithium salt. The conductivity of this copolymeric salt was measured to be 1.4×10^{-9} S cm^{-1}. Suspensions of the copolymeric salt were prepared in four insulating oils (silicone oil, mineral oil, trioctyl trimellitate, and dioctyl phatalate) in a series of concentrations (5–33%, m/m). The gravitational stabilities of these suspensions were determined at 20 and 80°C. The flow times of the suspensions were measured under no electric field (electric field strength = 0) and under an applied electric field (electric field strength ≠ 0), and the electrorheological activity was observed. Furthermore, the effects of the solid particle concentration, the shear rate, the electric field strength, a high temperature, and the addition of promoters on the electrorheological activities of the suspensions were investigated, and the excess shear stresses were determined. © 2003 Wiley Periodicals, Inc. J Appl Polym Sci 91: 1822–1833, 2004

Key words: rheology; ionomers; dispersions

INTRODUCTION

Considerable scientific and industrial interest is currently focused on a class of materials known as electrorheological (ER) fluids, which display remarkable rheological behavior, being able to convert rapidly and repeatedly from a liquid to a solid when an electric field is applied or removed.

The ER phenomenon was first reported by Winslow in 1949.[1] It is concerned with the influence of an electric field on the rheology of fluid dispersions, and it manifests itself in an increase in the resistance to flow and, in some cases, in the conversion of a fluid into a solid-like material. The number of investigations of ER fluids increased dramatically in the 1980s, and they were recently reviewed in numerous publications.[2–4] ER fluids can contain suspensions of polar particles in insulating liquids at solid volume fractions ranging from 5 to 50%.[5] ER fluids have considerable potential use in hydraulic control fluids, vibration damping systems, robotics, couplings, and automotive applications (i.e., electronically controlled shock absorbers, engine mounts, clutches, brakes, alternators, power-steering pumps, control valves, and artificial joints).[4,6,7]

Attention has recently been paid to the synthesis and characterization of various anhydrous (dry-base) ER systems. These systems can overcome several shortcomings of hydrous (wet-base) systems, such as the temperature limitation (caused by the presence of water or other polar promoters), the density mismatch between the particle and the oil, and the insufficient yield stress.[8] Among the various polarizable particles studied, semiconducting polymers, such as poly(acenequinone) radicals,[2] polyaniline,[9,10] and polypyrrole,[11,12] have been adopted as dry ER fluids with superior physical properties.[13]

The use of polymers as dispersed particles in high-performance ER fluids is now becoming common because of their low density, high plasticity, and easy processability into fine particles,[14] and they also have other advantages, such as a low zero-field viscosity [$\eta_{E=0}$; i.e., the viscosity at an electric field strength (E) of 0 kV/mm], nonabrasiveness, a wide effective temperature range, high colloidal stability against sedimentation, and redispersibility.[15]

For this purpose, poly(methacrylic acid), poly(acrylic acid)s, and their esters,[12] liquid-crystal polymers,[16] and semiconducting polymers[2,9–12,17] have been reported in the literature. In a number of cases, a polymer contained acid or other functional groups

Correspondence to: H. I. Ünal (hiunal@gazi.edu.tr).
Contract grant sponsor: Scientific and Technical Research Council of Turkey; contract grant number: TBAG-1485.

Journal of Applied Polymer Science, Vol. 91, 1822–1833 (2004)

introduced by chemical modification or by the addition of molecular acids.[18] The use of polymer fillers, in the H^+ form and as Li^+, K^+, Na^+, NH_4^+, and other salts, was shown to improve ER sensitivity, and Li^+ was found to be the best ion among the ions studied.[18–20]

Previously, we studied the ER properties of the poly(*tert*-butyl acrylate-*stat*-lithium acrylate)-*block*-polyisoprene copolymer system in pentaerythritol heptanoate and the polyisoprene-*block*-poly(carboxylithium styrene) copolymer system in silicone oil (SO); they formed micellar colloidal systems and showed ER activity and greater colloidal stability, and their ER activities were insensitive to the presence of trace moisture.[19,20]

In this study, promoter-free ER suspensions were prepared from the lithium salt of polyisoprene-*co*-poly(*tert*-butyl methacrylate) (PI-*co*-PTBMA-Li) in four insulating oils. The polymer was chosen for this study because it could be expected to associate in solution and form micellar particles with a core of poly(lithium-*tert*-butyl methacrylate) (PTBMA-Li) and an outer flexible fringe of polyisoprene (PI). This investigation was undertaken to provide additional information on the ER properties of copolymers, which have not been sufficiently discussed in the literature. Our attention especially focused on the following areas: the partial hydrolysis and salt formation of the poly(*tert*-butyl methacrylate) (PTBMA) part of the copolymer, the sedimentation stabilities and electrical properties of the suspensions, and the effects of the amounts of the polymeric particles, the presence of promoters, and high-temperature conditions.

EXPERIMENTAL

Materials

Isoprene (BDH) was stirred in the dark with crushed CaH_2 under a nitrogen atmosphere for 96 h and vacuum-distilled into a break-seal ampule from its living polymer solution initiated with *n*-butyllithium. *tert*-Butyl methacrylate (TBMA) was synthesized in our laboratory. Azobisisobutyronitrile (AIBN; BDH) was recrystallized twice from a nitric acid solution. Tetrahydrofuran (THF; Merck, Darmstadt, Germany) purification was performed *in vacuo* in the polymerization vessel. All other chemicals were used as received (Aldrich, Taufkirchen, Germany; analar grade).

Polymerization

The copolymer was prepared by radical polymerization with THF as a solvent and AIBN as an initiator. The first monomer, isoprene, was added to the polymerization vessel and stirred at 80°C under an $N_{2(gas)}$ atmosphere for 2 h; the second monomer, TBMA, was added dropwise into the living homo-PI solution, and the mixture was stirred for another 24 h at 80°C under an $N_{2(gas)}$ atmosphere. The copolymer was recovered by precipitation in excess methanol. Then, it was dried in a vacuum oven at 40°C for 48 h.

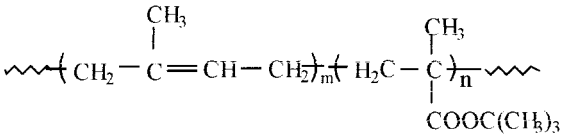

Scheme 1 Schematic representation of the copolymer structure (m = 103, n = 35).

Fractionation

Homo-PI and the low-molecular-weight copolymer were removed from the copolymer by liquid–liquid fractionation with toluene/methanol as the solvent/nonsolvent system at 20°C.

Characterization of the copolymer

Gel permeation chromatography (GPC, Waters, Milford, MA) was carried out at 25°C with THF as solvent at a flow rate of 10 cm^3/min with two Waters μ-Styragel columns (HR2+HTGE) and a Waters 410 refractive-index detector. The end-group analysis was performed through the titration of ester units of the copolymer with 0.1*M* aqueous NaOH. The Fourier transform infrared (FTIR) spectrum of the copolymer was recorded with a Mattson model 1000 FTIR spectrometer (Afi Unicam Ltd., Cambridge, UK). The samples were analyzed as films cast from dichloromethane onto a sodium chloride plate. The intrinsic viscosity measurements of the copolymer were performed in toluene with a Ubbelohde capillary flow viscometer mounted in a water bath maintained at 25.00 ± 0.01°C.

The elemental analysis was performed by the Turkish Scientific and Technical Research Council microanalytical laboratory, and the results were used as a check for purity, by comparison with the calculated composition, according to the structure given in Scheme 1. The ^{1}H-NMR spectrum was obtained in dimethyl sulfoxide-d_6 (DMSO-d_6) at the ambient temperature with a Bruker DPX Avonce 400-MHz nuclear magnetic resonance spectrometer (California) at the Turkish Scientific and Technical Research Council research laboratory.

Partial hydrolysis of the copolymer

The copolymer was dissolved in toluene, and then *p*-toluene sulfonic acid monohydrate (PTSA · H_2O) was added to this solution; the solution was stirred under a nitrogen atmosphere for 30 min. The solution was then transferred to a separating funnel and

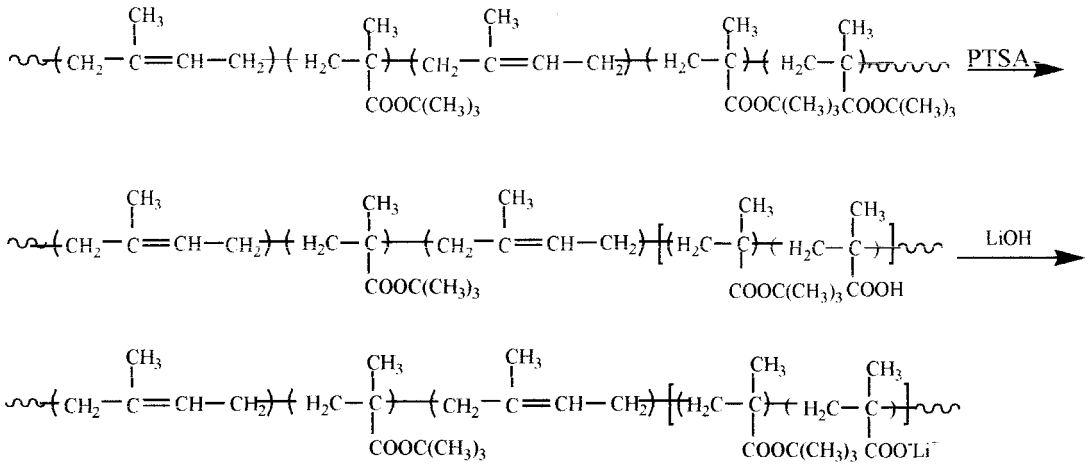

Scheme 2 Partial hydrolysis and salt formation reaction mechanism of the copolymer.

washed with 100-cm^3 of 0.1*M* aqueous LiOH to remove the residual PTSA from the reaction medium. This organic phase was also washed with distilled water to remove any residual lithium hydroxide. The product was dried in a vacuum oven at room temperature for at least 72 h. The reaction mechanism for the partial hydrolysis of the copolymer and the formation of the lithium salt are described in Scheme 2.

Characterization of the copolymeric salt

The elemental analysis of the copolymeric salt was also performed by the Turkish Scientific and Technical Research Council microanalytical laboratory, and the results were used to check the degree of hydrolysis and the percentage conversion to the lithium salt.

The particle size of the samples was determined by Fraunhofer scattering with a Malvern Mastersizer E (version 1.2b) particle size analyzer (Arkansas). During the measurements, the samples were dispersed in distilled water and stirred at a constant temperature of 20°C. The data collected were evaluated with Malvern software according to the Fraunhafer diffraction theory.[21] From the measurements, the average diameter of the particles was determined to be 45 μm.

The current–potential measurements were performed on a copolymeric salt disc (20 mm long, 5 mm wide, and 1 mm thick) with a Keithley 220 programmable current source and a Keithley 199 digital multimeter (Ohio) at the ambient temperature.

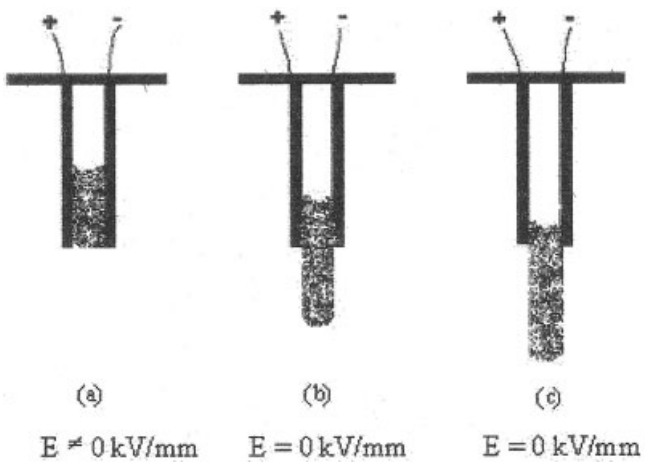

Scheme 3 Apparatus used to study the effect of the direct-current electric field on the flow behavior: (a) the fluid retained when the electric field is applied and (b,c) the flow occurring after the field is switched off.

Preparation of the suspensions

The suspensions of the copolymeric salt PI-*co*-PTBMA-Li were prepared in four insulating oils [silicone oil (SO), mineral oil (MO), trioctyl trimellitate (TOTM), and dioctyl phatalate (DOP)] at a series of concentrations (5–33%, m/m) by the dispersion of definite amounts of the copolymeric salt in calculated amounts of oil:

$$\text{m/m (\%)} = [m_{\text{copolymer}}/(m_{\text{copolymer}} + m_{\text{oil}})] \times 100 \quad (1)$$

TABLE I
Chemical Shifts Obtained for PI-*co*-PTBMA by ^{1}H-NMR Spectroscopy in DMSO-d_6

Assignment	Chemical shifts (δ, ppm)
TBMA, —C(C<u>H</u>$_3$)$_3$	1.6 s
Isoprene and TBMA, —C<u>H</u>$_3$	1.7–1.8 s
TBMA, —C<u>H</u>$_2$	2.4–3.6 t
Isoprene, —C<u>H</u>$_2$	5.6–5.8 m
Isoprene, —C<u>H</u>	6.6 t

s = singlet; m = multiplet; t = triplet.

TABLE II
Elemental Analysis Results of PI-*co*-PTBMA and PI-*co*-PTBMA-Li

		C (%)	H (%)	O (%)	Li (%)
PI-*co*-PTBMA	Calcd	79.7	11.0	9.3	—
	Found	79.4	10.9	9.7	—
PI-*co*-PTBMA-Li	Calcd	78.4	10.6	9.9	1.1
	Found	78.3	10.3	10.1	1.3

Determination of the sedimentation stability of the suspensions

The sedimentation stabilities of the suspensions, prepared in four insulating oils, were determined at two different temperatures (20 and 80°C) by the immersion of glass tubes, containing the suspensions, in a water bath. The formation of the first precipitates was taken to be an indication of sedimentation instability.

Rheometry

Rheological experiments were carried out for the suspensions prepared in four insulating oils for the experimental determination of the flow behavior and viscoelastic material properties, which influence the processing technology and polymer stability and consistency.

Flow rate measurements were carried out between two brass electrodes, as illustrated in Scheme 3. The gap between the electrodes was 0.5 cm, the width of the electrodes was 1.0 cm, and the height of the liquid on the electrodes was 5.0 cm. During the measurements, these electrodes were connected to a high-voltage direct-current electric source and a voltmeter. At the beginning of the experiment, the electrodes were dipped into a vessel containing the ER fluid, and after a few seconds, the vessel was removed and the flow time for complete drainage was measured with a digital stopwatch. During the second stage, the electrodes were again dipped into the same vessel containing the ER fluid, and stepwise electric fields were applied above the yield point, perpendicularly to the electrodes. After several seconds, the vessel was removed, and the flow time for complete drainage was measured under the applied electric field ($E \neq 0$). This procedure was repeated for each ER fluid concentration under various field strengths.

Rotational viscometry was carried out at two different temperatures, 20 and 80°C. The shear rates ($\dot{\gamma}$) used were relatively low (0.1–20 s^{-1}) because of instrumental limitations. For measuring the viscosity of a liquid, a spindle was simply immersed in the liquid container, the motor was switched on, and the viscosity was read on the calibrated dial of the instrument. For measuring the viscosity of the suspensions under an applied electric field, those parallel-plate electrodes were immersed in the fluid container, the 5.0-mm gap between the brass electrodes was kept constant, an electric field was created in the fluid, and the spindle was forced to rotate. The voltage used in these experiments was supplied by a 0–10-kV (with 0.1 kV/mm increments) direct-current electric field generator, which enabled resistivity to be created during the experiments.

RESULTS AND DISCUSSION

Characterization

Polyisoprene-*co*-poly(*tert*-butyl methacrylate) (PI-*co*-PTBMA) was prepared by radical polymerization. It was partially hydrolyzed and converted into the lithium salt PI-*co*-PTBMA-Li. The characterization of PI-*co*-PTBMA and PI-*co*-PTBMA-Li is discussed later. From GPC chromatograms, the polystyrene-equivalent number-average molar masses of the PI precursor and PI-*co*-PTBMA were determined to be 7000 and 12,000 g/mol, respectively. From end-group analysis, the number-average molar mass of the acrylate units was determined to be 5000 g/mol, which agrees very well with the molar mass difference of the copolymer and PI obtained from GPC.

The intrinsic viscosities of PI-*co*-PTBMA and PI-*co*-PTBMA-Li were determined by extrapolation to infinite dilution from plots of $\ln \eta_r/c$ and η_{sp}/c (where η_r and η_{sp} are the relative and specific viscosities, respectively, and c is the concentration) against the concentration and were found to be 0.25 and 0.14 dm^3/g, respectively. The polymeric salt reached a lower value of $\eta_{E=0}$ after partial hydrolysis and salt formation. The data obtained from the ^{1}H-NMR spectrum of PI-*co*-

TABLE III
Sedimentation Stability Results of PI-*co*-PTBMA-Li Suspensions in Four Insulating Oils

Concentration (m/m)	Sedimentation stability											
	33%		25%		20%		15%		10%		5%	
Temperature	20°C	80°C	20°C	80°C	20°C	80°C	20°C	80°C	20°C	80°C	20°C	80°C
SO	16 days	19 days	17 days	20 days	19 days	23 days	24 days	27 days	38 days	39 days	54 days	57 days
DOP	1 h	1 h	3 h	3 h	4 h	5 h	5 h	7 h	7 h	9 h	12 h	15 h
TOTM	2 days	2 days	2 days	3 days	4 days	4 days	5 days	6 days	6 days	8 days	10 days	14 days
MO	8 days	8 days	9 days	10 days	12 days	14 days	12 days	15 days	17 days	19 days	32 days	35 days

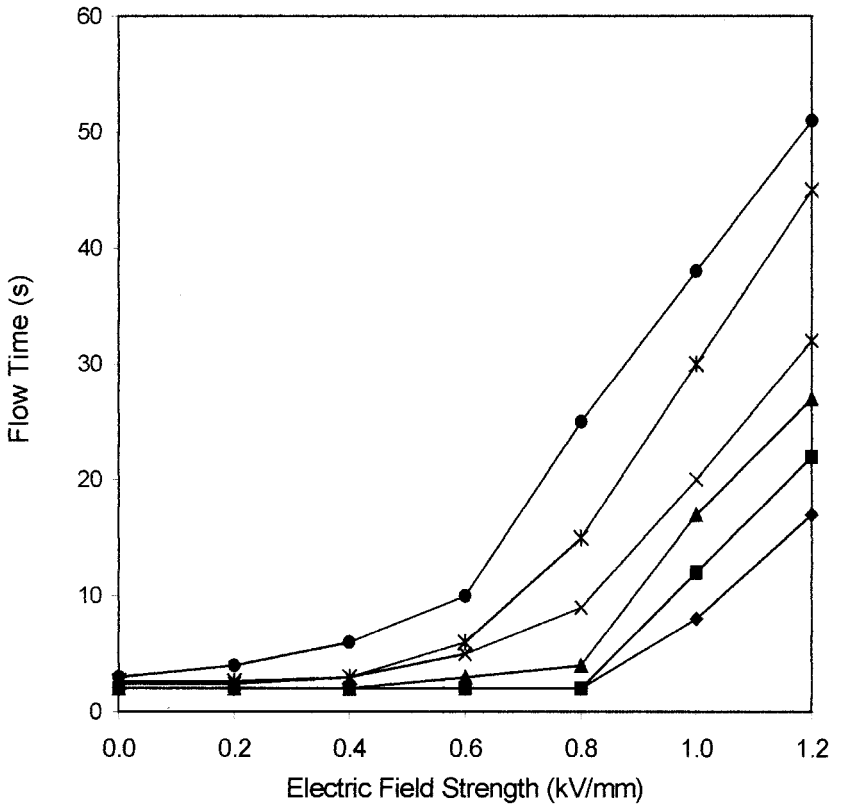

Figure 1 Changes in the flow times with *E*. The dispersion medium was SO, and the concentrations were (♦) 5, (■) 10, (▲) 15, (×) 20, (∗) 25, and (●) 33% (m/m).

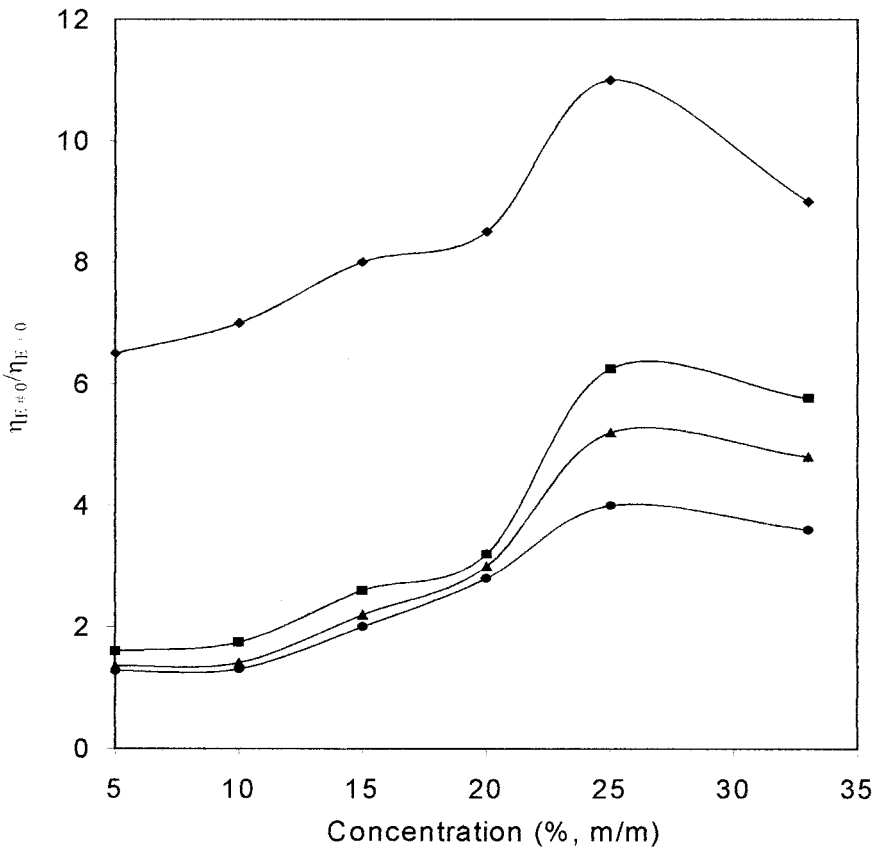

Figure 2 Changes in the viscosity with the concentration. The temperature was 20°C, *E* was 0–1 kV/mm, and the dispersion medium was SO. The $\dot{\gamma}$ values were (♦) 1, (■) 4, (▲) 10, and (●) 20 s^{-1}.

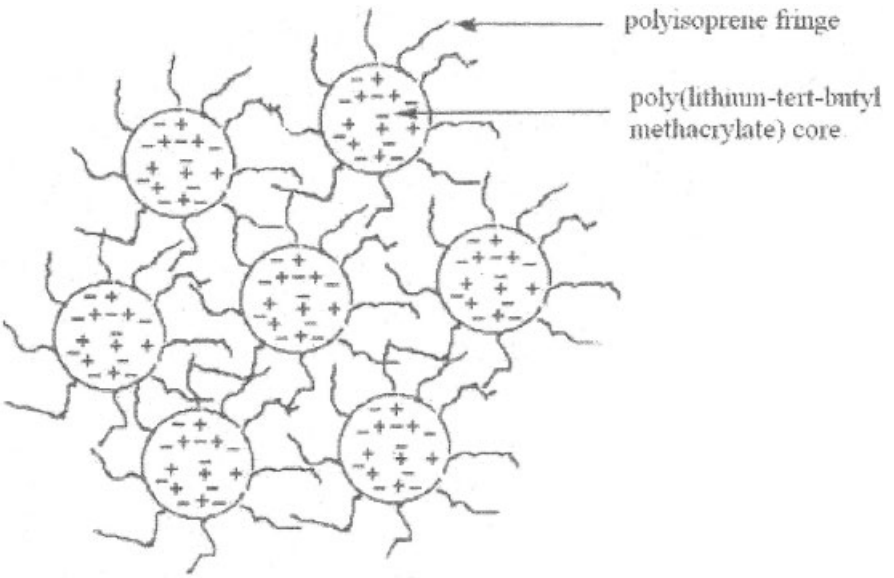

Figure 3 Illustration of micellar aggregates formed by PI-*co*-PTBMA-Li in SO.

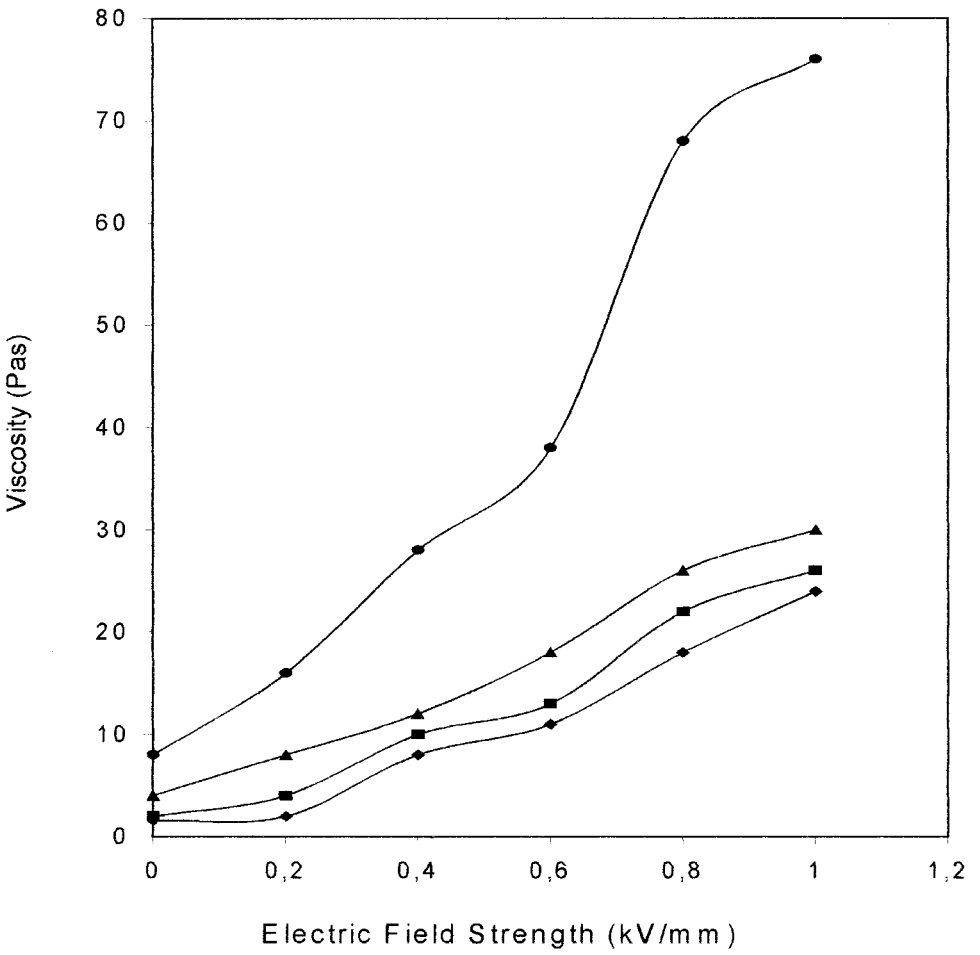

Figure 4 Changes in the viscosity with E. The temperature was 20°C, the concentration was 25%, and the dispersion medium was SO. The $\dot{\gamma}$ values were (●) 1, (▲) 4, (■) 10, and (♦) 20 s^{-1}.

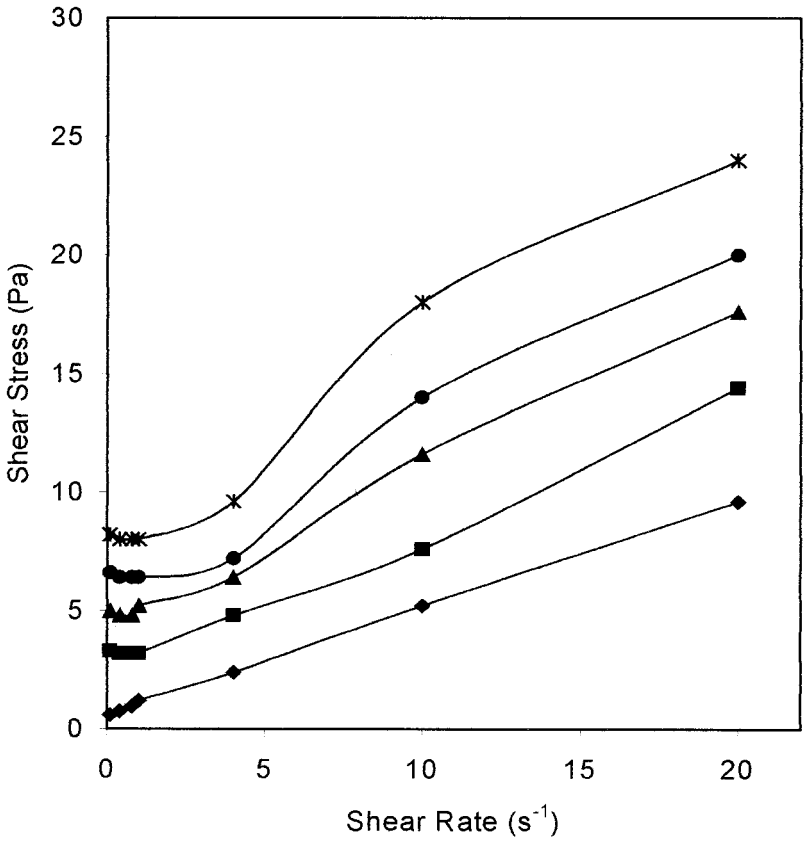

Figure 5 Changes in τ with the shear rate. The temperature was 20°C, the concentration was 25% (m/m), and the dispersion medium was SO. The E values were (♦) 0.0, (■) 0.20, (▲) 0.4, (●) 0.8, and (∗) 1.0 kV/mm.

PTBMA contained peaks that could be assigned to PI and PTBMA units. The chemical shifts of particular groups in PI-*co*-PTBMA are given in Table I, in view of the structure given in Scheme 2, although ^{1}H-NMR data contained peaks corresponding to both 1,4- and 3,4-additions of PI units.

The FTIR spectrum of PI-*co*-PTBMA showed the expected distinctive absorptions. The absorptions at 1740, 1240, 1600, 2920, and 1400 cm^{-1} are typical of —C═O, ether stretching C—O—C, aliphatic C—H stretching, C—H bending due to CH_3 absorptions, and C═C stretching, respectively. The hydrolyzed copolymer gave an FTIR spectrum similar to that of PI-*co*-PTBMA with an additional peak at 3400 cm^{-1} due to O—H binding of hydrolyzed PI-*co*-PTBMA. PI-*co*-PTBMA-Li also gave an FTIR spectrum similar to that of PI-*co*-PTBMA.

The experimental and calculated compositions, obtained from an elemental analysis of PI-*co*-PTBMA and PI-*co*-PTBMA-Li, are shown in Table II. The measured compositions agree very well with the calculated values. These results also prove that the copolymer was successfully partially hydrolyzed and converted into the Li salt.

The conductivity of PI-*co*-PTBMA-Li was measured to be 1.4×10^{-9} Scm^{-1}, which is in the range of conductivity of ER particles.[4] This low conductivity value is due to the low ion content of the copolymeric salt (1.3% Li ion). As expected, the driving force behind the ER activity of this copolymeric salt/insulating oil system is the migration of ionomeric particles suspended inside the suspensions.

Sedimentation stability

The sedimentation stabilities of PI-*co*-PTBMA-Li suspensions were determined in four insulating oils at 20 and 80°C, before ER measurements were carried out, and the results obtained are tabulated in Table III. The sedimentation stabilities of suspensions increased with both decreasing particle concentration and increasing temperature, as expected. The maximum sedimentation stability was found to be 57 days at a 5% suspension concentration in SO at 80°C. The sedimentation stabilities of the suspensions increased in the following order: DOP < TOTM < MO < SO.

Electrorheology: flow measurements

The flow times of PI-*co*-PTBMA-Li suspensions measured between the parallel-plate electrodes at E = 0.0 kV/mm and at E = 0.0–2.0 kV/mm are shown

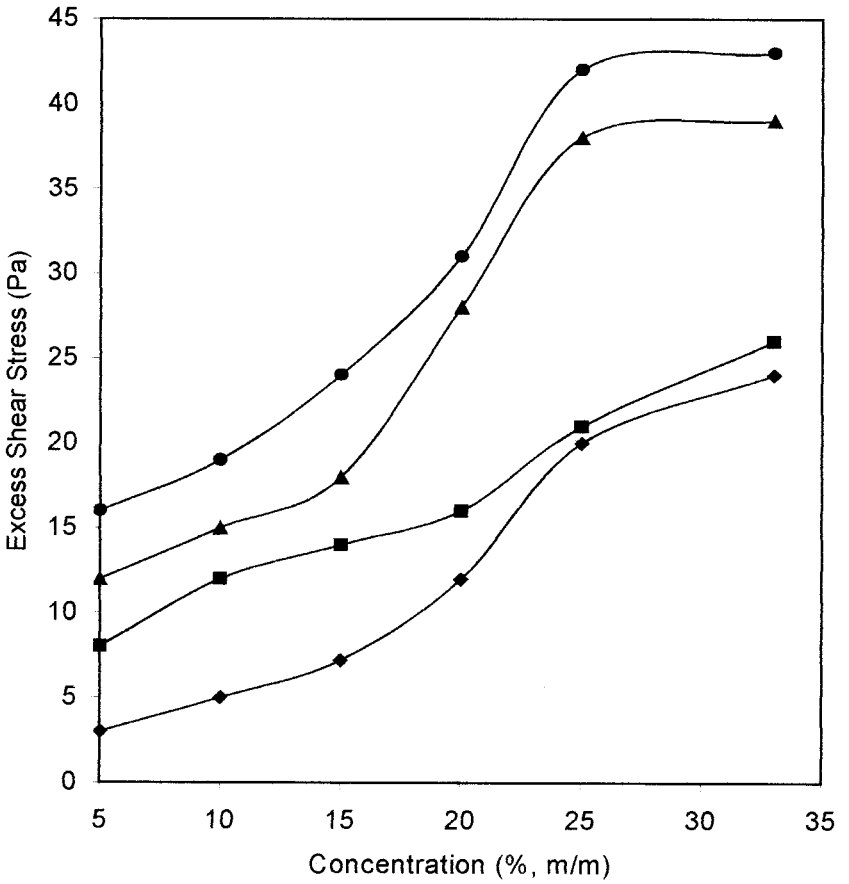

Figure 6 Changes in $\Delta\tau$ with the concentration. $\dot{\gamma}$ was 20 s^{-1}, the temperature was 20°C, and E was 0.0 or 1.0 kV/mm. The dispersion media were (●) SO, (▲) TOTM, (■) MO, and (♦) DOP.

in Figure 1. The flow times of the suspensions increased as E and the suspension concentration increased. The highest flow time (51 s) was obtained with a 33% suspension concentration at E = 1.2 kV/mm in SO. The flow times illustrated in Figure 1 are the maximum flow times measured at E = 1.2 kV/mm. When E was further increased, the flow of the liquid between the electrodes was completely stopped, and measurements could not be made even after 24 h. The same measurements were carried out for the suspensions prepared in the other three insulating oils, and similar trends were observed. The maximum flow times of the suspensions varied in the following order: SO (51 s) > TOTM (41 s) > MO (40 s) > DOP (35 s). This may be attributed to (1) differences between the physical properties of the insulating oils, such as the density and viscosity,[12] and (2) different intermolecular interactions acting between these insulating oils and the ionomer particles. The flow times given for the suspensions are the maximum flow times observed under an applied electric field of 1.2 kV/mm. When E was further increased, a stronger bridge formation occurred for all the suspensions, and no flow was observed. Similar behavior was reported for polystyryllithium-*block*-polyisoprene copolymeric salt[20] and alumina[22] suspensions in SO.

Rotational viscometry

Effect of the particle concentration on the electric field viscosity ($\eta_{E\neq0}$)

The ratio of $\eta_{E\neq0}$ to $\eta_{E=0}$ has been plotted as a function of the particle concentration for PI-*co*-PTBMA-Li suspensions in Figure 2. The suspension concentration exerts the principle effect on the ER effect. $\eta_{E\neq0}/\eta_{E=0}$ increases with increasing particle concentration up to 25% and then decreases. We suppose that PI-*co*-PTBMA-Li particles formed the core–shell micellar structure in SO as illustrated in Figure 3. The core was PTBMA-Li salt, and the shell was PI. The ion–dipole interaction between the PTBMA-Li core and PI fringe offered strong adhesion between the core and shell of the particles. The core exhibited ion migration between the particles, and this resulted in increasing polarization of the particles, hence raising the viscosity of the suspension. The magnitude of this polariza-

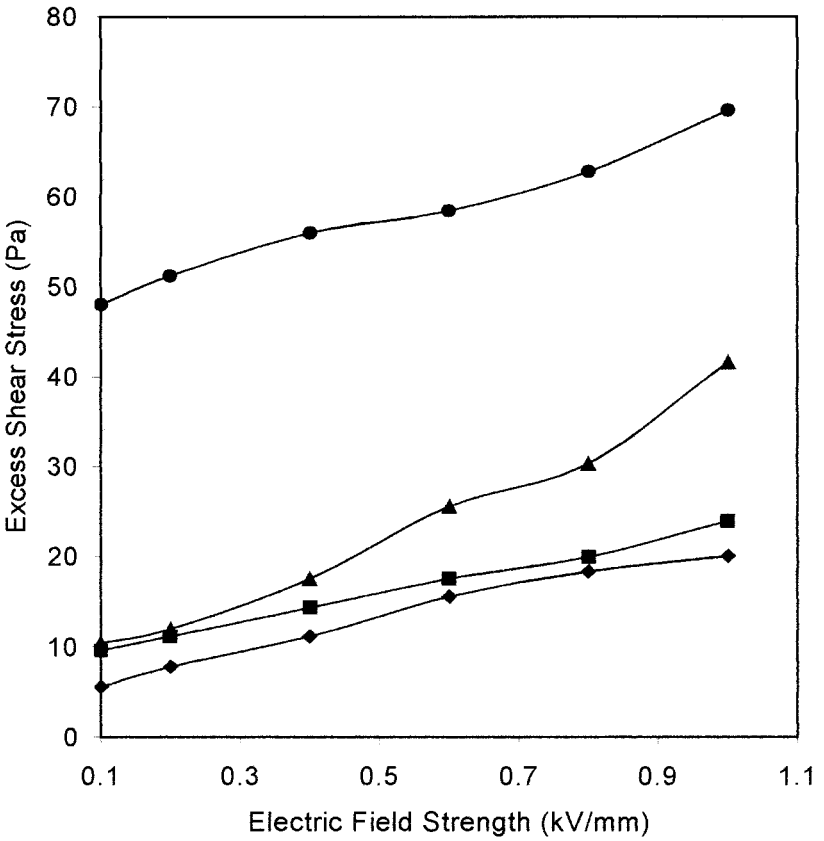

Figure 7 Changes in $\Delta\tau$ with E. $\dot{\gamma}$ was 20 s^{-1}, the temperature was 20°C, and the concentration was 25%. The dispersion media were (●) SO, (▲) TOTM, (■) MO, and (♦) DOP.

tion force (F_p) in the direction of the applied electric field (E) is[23]

$$F_p = 6\varepsilon_2 r^6 E^2/\rho^4 \quad (2)$$

where ϵ_2 is the dielectric constant of the particles, ρ is the distance between particles, and r is the radius of a particle. As reflected from eq. (2) the distance between the particles decreases with increasing suspension concentration, and this results in increased F_p and $\eta_{E\neq 0}$.

Wu and Shen[24] reported an 11% optimum concentration in the ER studies of chitin and chitosan suspensions in SO, and Kordonsky et al.[18] reported a 20% optimum concentration in the ER studies of carboxy methylcellulose suspensions in transformer oil.

Effects of E on the viscosity

Figure 4 shows the change in the viscosity with E for the PI-*co*-PTBMA-Li/SO system at various values of ($\dot{\gamma}$) = (1–20 s^{-1}) and a 25% optimum suspension concentration. The increase in the ER activity of the suspensions is directly proportional to the increase in E and is inversely proportional to $\dot{\gamma}$. Under an applied electric field, the magnitude of the polarization forces between particles increases with increasing field strength, and this, in turn, increases the chain length (formed by particles), thus resulting in the enhancement of the viscosity of the suspension. PI-*co*-PTBMA-Li particles are affected by the hydrodynamic interactions and the viscous forces (F_η), which have the following magnitude:[24]

$$F_\eta = 6\pi\eta_s r^6 \dot{\gamma} \quad (3)$$

where η_s is the viscosity of the suspension and $\dot{\gamma}$ is the average shear rate. As $\dot{\gamma}$ increases, the viscous forces increase, and so the tendency to break down the structural skeleton of the suspension is increased. Therefore, the suspension structure that forms because of the applied electric field is much easier to damage, and the increment of the viscosity is much smaller. However, at higher shear rates, the suspension viscosity becomes less dependent of on E. This suggests that, at high shear rates, the viscous forces are dominant, and the suspension structure does not vary appreciably with E.[24] A similar trend was observed by Wu and Shen[24] in ER studies of chitin and chitosan suspensions prepared in SO and by Pavlinek et al.[25] in ER studies of poly(glycidyl methacrylate) suspensions prepared in SO.

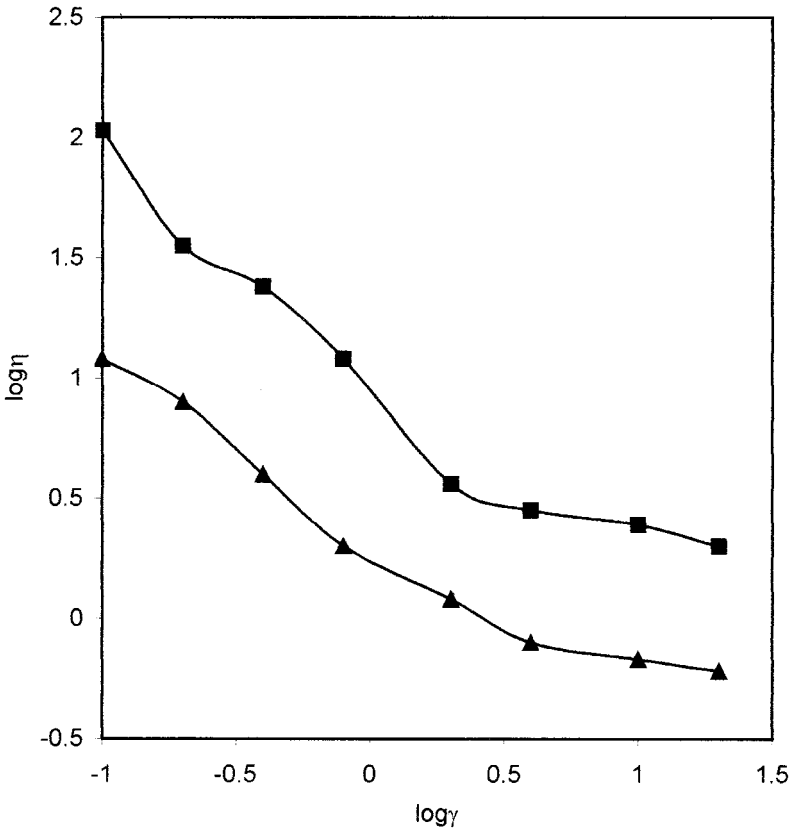

Figure 8 Changes in the viscosity with the shear rate. The temperature was 20°C, the concentration was 25%, and the dispersion medium was SO. *E* was (▲) 0.0 or (■) 1.0 kV/mm.

Change in the shear stress (τ) with the shear rate

The PI-*co*-PTBMA-Li/SO suspension's τ value as a function of the shear rate at different field strengths and the optimum concentration (25%) is shown in Figure 5. In the absence of an electric field (E = 0.0 kV/mm), τ– $\dot{\gamma}$ curves appear almost linear. τ increases significantly with an increase in the shear rates, and this can be attributed to the viscous forces, which control the suspension's structure.[26]

A similar trend was observed by Orihara et al.[27] in ER studies of liquid-crystal polymer blend suspensions prepared in SO.

Change in the excess shear stress ($\Delta\tau$) with the concentration

In Figure 6, it can be seen that $\Delta\tau$ ($\tau_{E\neq0} - \tau_{E=0}$) is a function of the particle concentration at constant values of $\dot{\gamma}$ (20 s^{-1}) and E (1.0 kV/mm). $\Delta\tau$ rapidly increases with increasing particle concentration up to 25% and reaches a plateau region at large concentrations, especially in TOTM and SO suspensions. At low concentrations, $\Delta\tau$ increases with increasing concentration. This is because of the increasing interparticle interaction (polarization force) resulting from the increasing concentration, which, in turn, strengthens the system structure. Similar behavior was reported by Xie and Guan[28] for a polyaniline suspension prepared in SO.

Change in $\Delta\tau$ with E

Figure 7 shows the dependence of $\Delta\tau$ on E at a 25% particle concentration of the copolymeric salt in the four insulating oils. As shown in Figure 6, $\Delta\tau$ increases with applied E, and this may be attributed to the increased magnitude of polarization forces with increasing E. A similar trend was reported by Otsubo and Edamura[29] in ER studies of 1,3-ethylene gylcol dimethacrylate-*block*-butyl acrylate copolymer suspensions in SO and by Xie and Guan[30] in ER studies of polyaniline suspensions in silicone and paraffin oils.

Effect of the shear rate and temperature on the viscosity

Changes in the log viscosity of a suspension with the log shear rate at the optimum suspension concentration (25%) in SO are shown in Figure 8. With and without applied E, the viscosity of the suspension decreases sharply with an increasing shear rate, giving a typical curve of shear-thinning non-Newtonian vis-

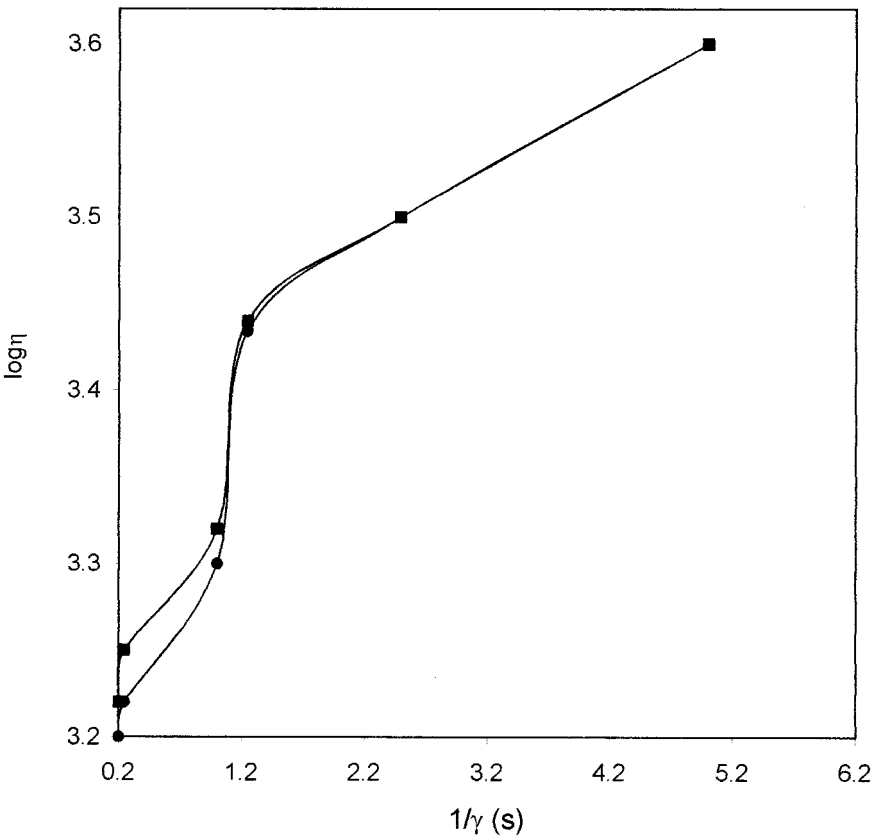

Figure 9 Changes in the viscosity with the temperature and shear rate. *E* was 1.0 kV/mm, the dispersion medium was SO, and the concentration was 25%. The temperature was (●) 20 or (■) 80°C.

coelastic behavior.[31] An analogous trend was observed for copolymeric salt suspensions prepared in the other three oils. Similar results were reported for studies of poly(lithium-2-acrylamido-2-methyl propane sulfonic acid),[32] polyaniline,[33] and magnesium hydroxide solutions,[34] all prepared in SO.

The variability of the ER activity with the temperature is known to be a major problem for most conventional ER fluids and can limit their high-temperature use.[33,35] In Figure 9, changes in the viscosity with the shear rate are presented at two different temperatures (20 and 80°C). Log η increases with $1/\dot{\gamma}$. From these observations, we may conclude that the PI-*co*-PT-BMA-Li SO ER active system is not affected by the high temperatures within the limits studied.

Effect of the promoter on the ER activity

The influence of moisture on the ER activity was also investigated through the addition of polar solvents (i.e., water, ethanol, ethanol amine, glycerol, and sodium lauryl sulfate) at 100–1000 ppm (with 100 ppm increments) to the copolymeric salt suspensions (concentration = 25%, m/m). The suspensions of the copolymeric salt prepared in SO, MO, and DOP were not sensitive to the amount of moisture present over the range studied. However, the suspensions prepared in TOTM showed electrical breakdown when subjected to a high electric field after the addition of any promoter. The variability of the ER activity with the temperature and moisture content is known to be a major problem for most conventional ER fluids and can limit their high-temperature use.[36] The observation that the copolymeric system investigated in this work is not affected by the addition of a promoter and high temperatures could prove particularly important for industrial applications.

CONCLUSIONS

1. The sedimentation stability of a polymeric salt in SO was found to be 57 days at a 5% suspension concentration and decreased in the order of SO > MO > TOTM > DOP.
2. The flow times of the suspensions were observed to increase as *E* and the suspension concentration increased. The highest flow time (51 s) was obtained at a 33% suspension concentration at *E* = 1.4 kV/mm.
3. The viscosity ratio ($\eta_{E\neq0}/\eta_{E=0}$) increased up to a 25% suspension concentration and then decreased.

4. The ER activities of the suspensions increased as the field strength increased and the shear rate decreased.
5. Excess shear stresses sharply increased as the field strength and suspension concentration increased.
6. The viscosity of the suspensions decreased sharply as the shear rate increased, presenting typical shear-thinning non-Newtonian viscoelastic behavior.
7. The copolymeric salt system was insensitive to high temperatures and moisture within the limits studied.

The authors are grateful to Süleyman Saritas for the particle size measurements.

References

1. Winslow, W. M. J Appl Phys 1949, 20, 1137.
2. Block, H.; Kelly, J. P. J Phys D: Appl Phys 1988, 21, 1661.
3. Block, H. In Polymers in Solution; Forsman, W. C., Ed.; Plenum: New York, 1986.
4. Hao, T. Adv Colloid Interface Sci 2002, 97, 1.
5. Hasley, T. C.; Torr, W. Phys Rev Lett 1990, 65, 2820.
6. Shulman, Z. P.; Gorodkin, R. G.; Korobko, E. V.; Gleb, V. K. J Non-Newtonian Fluids Mech 1981, 8, 29.
7. Tao, R.; Roy, G. D. In Electrorheological Fluids: Mechanisms, Properties, Technology and Applications; Tao, R.; Roy, G. D., Eds.; World Scientific: London, 1994; Chapter 4.
8. Kim, S. G.; Kim, J. W.; Jang, W. H.; Choi, H. J.; John, M. S. Polymer 2001, 42, 5005.
9. Chin, B. D.; Lee, Y. S.; Park, O. O. J Colloid Interface Sci 1998, 201, 172.
10. Gow, C. J.; Zukoski, C. F. J Colloid Interface Sci 1990, 126, 175.
11. Wu, S.; Zeng, F.; Shen, J. Polym J 1998, 30, 451.
12. Sahin, D.; Sari, B.; Ünal, H. I. Turk J Chem 2002, 26, 113.
13. Choi, H. J.; Kim, T. W.; Cho, M. S.; Kim, S. G.; John, M. S. Eur Polym J 1997, 33, 699.
14. Xie, H. Q.; Tian, D.; He, P.; Guo, J. J Appl Polym Sci 1998, 68, 2169.
15. Bloodworth, R. In Electrorheological Fluids: Mechanisms, Properties, Technology and Applications; Tao, R.; Roy, G. R., Eds.; World Scientific: Singapore, 1994; p 67.
16. Reyes, J. A.; Monero, O.; Rodriguez, R. F. Rheol Acta 2001, 40, 426.
17. Tanaka, K.; Orwa, Y.; Akiyama, R.; Kubano, A. Polym J 1998, 30, 171.
18. Kordonsky, V. I.; Korobko, E. V.; Lazareva, T. G. J Rheol 1991, 35, 1427.
19. Ünal, H. I. J Faculty Eng Arch Gazi Univ 1994, 9, 69.
20. Yavuz, M.; Ünal, H. I.; Yildirir, Y. Turk J Chem 2001, 25, 19.
21. German, R. M. Powder Metallurgy Science; Material Powder Industries Separation: Princeton, NJ, 1994; p 28.
22. Parthasarathy, M.; Klingenberg, D. J. Mater Sci Eng R 1996, 17, 57.
23. Bezruk, V. I.; Lazarev, A. N.; Malov, V. A.; Usyarov, O. G. Colloid J 1972, 34, 142.
24. Wu, S.; Shen, J. J Appl Polym Sci 1996, 60, 2159.
25. Pavlinek, V.; Quadrat, O.; Saha, P.; Benes, M. J.; Trlica, J. Colloid Polym Sci 1998, 276, 690.
26. Wu, S.; Lu, S.; Shen, J. Polym Int 1996, 41, 363.
27. Orihara, H.; Taki, A.; Doi, M. J Rheol 2001, 45, 1479.
28. Xie, H. Q.; Guan, J. G. Angew Makromol Chem 1996, 235, 21.
29. Otsubo, Y.; Edamura, K. J Rheol 1994, 38, 1721.
30. Xie, H. Q.; Guan, J. G. Angew Makromol Chem 1996, 231, 21.
31. Weiss, K. D.; Duclos, T. G. In Electrorheological Fluids: Mechanisms, Properties, Technology and Applications; Tao, R.; Roy, G. D., Eds.; World Scientific: London, 1994; p 43.
32. Ünal, H. I.; Yilmaz, H. J Appl Polym Sci 2002, 86, 1106.
33. Tanaka, K.; Orwa, Y. Polym J 1998, 30, 171.
34. Trlica, J.; Quadrat, O.; Bradna, P.; Pavlinek, V.; Saha, P. J Rheol 1996, 40, 943.
35. Xiong, C.; Wan, Y.; Wen, D. J. Wuan Univ Tech Mater Sci Ed 1997, 12, 41.
36. Rankin, P. J.; Klingenberg, D. J. J Rheol 1998, 42, 639.